# OAJ: 2.6m Wide Field Survey Telescope

Olivier Pirnay*, Vincent Moreau, Grégory Lousberg

Advanced Mechanical and Optical Systems (AMOS s.a.),
LIEGE science park, B-4031 Angleur, BELGIUM

## ABSTRACT

AMOS S.A. is in charge of the development of the telescopes for the "Observatorio Astrofisico de Javalambre" in Spain where a 2.6 m wide field telescope is complemented by an 80 cm telescope. This paper focuses on the 2.6 m telescope *Javalambre Survey Telescope* (JST): it is combining a large collecting surface with a wide field of view for reaching a vast portion of the sky, which is the most relevant parameter for surveys, while ensuring an optical image quality compatible with the site seeing and a suitable depth in the sky sighting.

The major difficulty consists in maintaining the image quality over a 500 mm focal plane. A good design is the result of a thorough multidisciplinary optimization process where the fabrication constraints are a major driving parameter. The complexity of the system led to elaborate innovative solutions for the closed loop control of both image quality and tracking features.

The design and the methodology of working are presented in details. The optics fabrication, the integration and acceptance tests are also reviewed.

**Keywords:** OAJ, JST, Javalambre Survey Telescope, Aspheric Optics, Wide Field, Curvature Wavefront Sensing.

## 1. INTRODUCTION

The *Centro de Estudios de Física del Cosmos de Aragón* (CEFCA) is a scientific foundation created in 2008. It is located in the region of Aragón, Spain. It aims at developing and operating an observatory dedicated to astronomical surveys in the Javalambre mountains. The selected site is the *Pico del Buitre* situated 1957 m above the sea level and 150 km West of the Mediterranean coast. A 2.6 m class telescope and an auxiliary 80 cm telescope are installed on the site almost at the same time.

The purpose of the new observatory is to provide state-of-the-art facilities for performing extensive campaigns of astrophysical sky survey, as required by the current developments in observational cosmology. It is by the way intended to benefit from the outstanding features of the Pico del Buitre site seeing to optimize the data retrieval rate and yield a leading place to this observatory in the universe scientific quest.

The 2.6m telescope or Javalambre Survey Telescope (JST) is combining a large collecting surface with a wide field of view for reaching a vast *étendue*, which is one of the most relevant parameter for surveys, while ensuring an optical imaging quality compatible with the site seeing and a suitable depth in the sky sighting. These features will greatly support the main scientific objectives of the project as part of an international cooperation for the creation of huge databases of observational data.

The JST is complemented by an 80 cm telescope which provides the radiometric/photometric calibrations needed for the optimization of the JST accuracy. Thanks to its earlier commissioning, this telescope will also serve as training equipment for the observatory personnel in the perspective of the JST.

*olivier.pirnay@amos.be; phone +32 4 361 40 40; www. amos.be

## 2. TELESCOPE SPECIFICATIONS

The top level requirement specifications of the JST are presented in Table 1. The key feature of the telescope is the fact that its forefront performances are combined with a large (FOV). Each step of the design required a multidisciplinary work always governed by these top-level specifications. The innovative design and the fabrication of challenging optics form the bedrock of such an ambitious technical project.

The telescope is almost devoted to survey program set-up in the frame of the J-PAS Collaboration. For this purpose, it will be operated together with a gigapixel mosaic camera composed of 14 CCD's of 10K×10K pixels combined with 14 individual filters.

Table 1. JST requirement specifications

| Item | Specification |
| --- | --- |
| Configuration | Ritchey-Chrétien with one axial Cassegrain focal plane<br>Equipped with a field corrector<br>Instrument adaptor with field de-rotator<br>Altitude – Azimuth mount |
| Aperture | 2.6 m diameter |
| Field of view | 3 deg (diameter) |
| Etendue | > 34 $m^2$ $deg^2$ |
| Plate scale | 22.67 arcsec / mm (44 µm/arcsec) |
| Focal length | 9098 mm (deduced from plate scale requirement) |
| Spectral bandwidth | 330-1100 nm |
| Image Quality | 50% EE <= 0.27 arcsec (diameter)<br>80% EE <= 0.41 arcsec (diameter) |
| Distortion | < 0.003 (with a goal at 0.0003) |
| Pointing accuracy | <= 2.5 arcsec RMS over the field of regard<br><= 0.5 arcsec RMS over 2 deg |
| Tracking accuracy | <= 0.18 arcsec RMS over 15 sec period<br><= 0.4 arcsec RMS over 5 min. period |
| Sky coverage | 1 to 70 deg from zenith |
| Slewing speed | 4 deg/sec and 1 $deg/sec^2$ |
| Rotator tracking | <=0.15 arcsec |
| Operational Environment | Wind <= 18 m/s<br>Temperature: -15°C to 25°C<br>HR <= 95% |

## 3. TELESCOPE OPTICS

### 3.1 Optical Layout

The telescope is derived from a Ritchey-Chrétien configuration with a Cassegrain focal plane. The lay-out is represented in Figure 1. The primary (M1) and secondary (M2) mirrors have aspheric surfaces. The telescope is equipped with a large field corrector that is located beyond the central hole of the primary mirror. The design takes into account the presence of 8 mm thick filters and a 25 mm thick plano-convex camera window in the optical path.

The primary is a f/1.5 concave 8th-order aspheric mirror made of ZERODUR® with a diameter of 2640 mm. It has a central hole of 1010 mm diameter and a thickness of 250 mm at the edge. The wavefront quality is 20 nm RMS WFE over the entire useful area and is better than 0.5 µrad RMS wavefront slope error for the defects in the range of 2 mm to 100 mm. The maximum departure from the best fitting sphere is 276 µm and 0.47 mrad in slope.

The secondary is a f/2.2 convex 6th order aspheric mirror made of ZERODUR®. The outside diameter is 1250 mm and the central thickness is 120 mm. The wavefront quality is 20 nm RMS WFE (astigmatism removed) over the entire useful area and better than 1 µrad RMS wavefront slope error for the defect in the range of 2 mm to 40 mm. The maximum departure from the best fitting sphere is 272 µm and 0.89 mrad in slope.

The field corrector is composed of 3 lenses of 600 mm diameter made of Suprasil® and with a center thickness of 30 to 55 mm: the first lens has two high order aspheric surfaces while the second and third lenses have one aspheric surface and a spherical one. These lenses are characterized by very short radius of curvature and extreme departure to the best sphere: up to 8 mm and 50 mrad for the first lens.

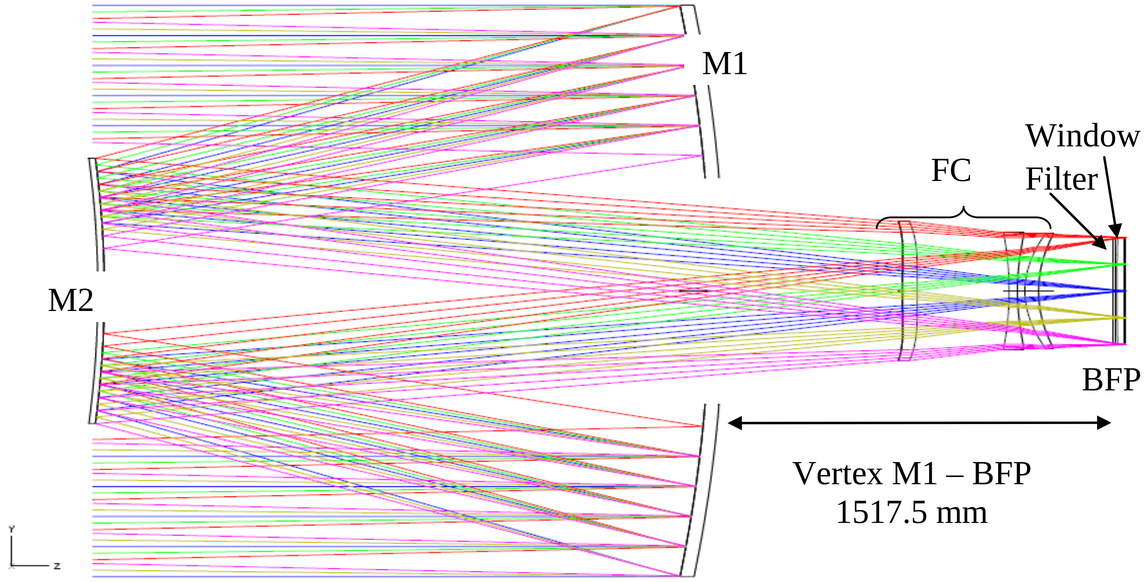

Figure 1. JST optical layout

The optical combination is optimized to get the best polychromatic image quality in the range of 330 nm to 1100 nm over the entire field of view. The diffractive encircle energy (EE) is evaluated for 11 narrow bands at 11 points in the field of view (Figure 3). The system cannot suffer a non-homogeneous image quality in both the spatial and wavelength range since a portion of the sky is observed sequentially by adjacent CCD covered by different filters.

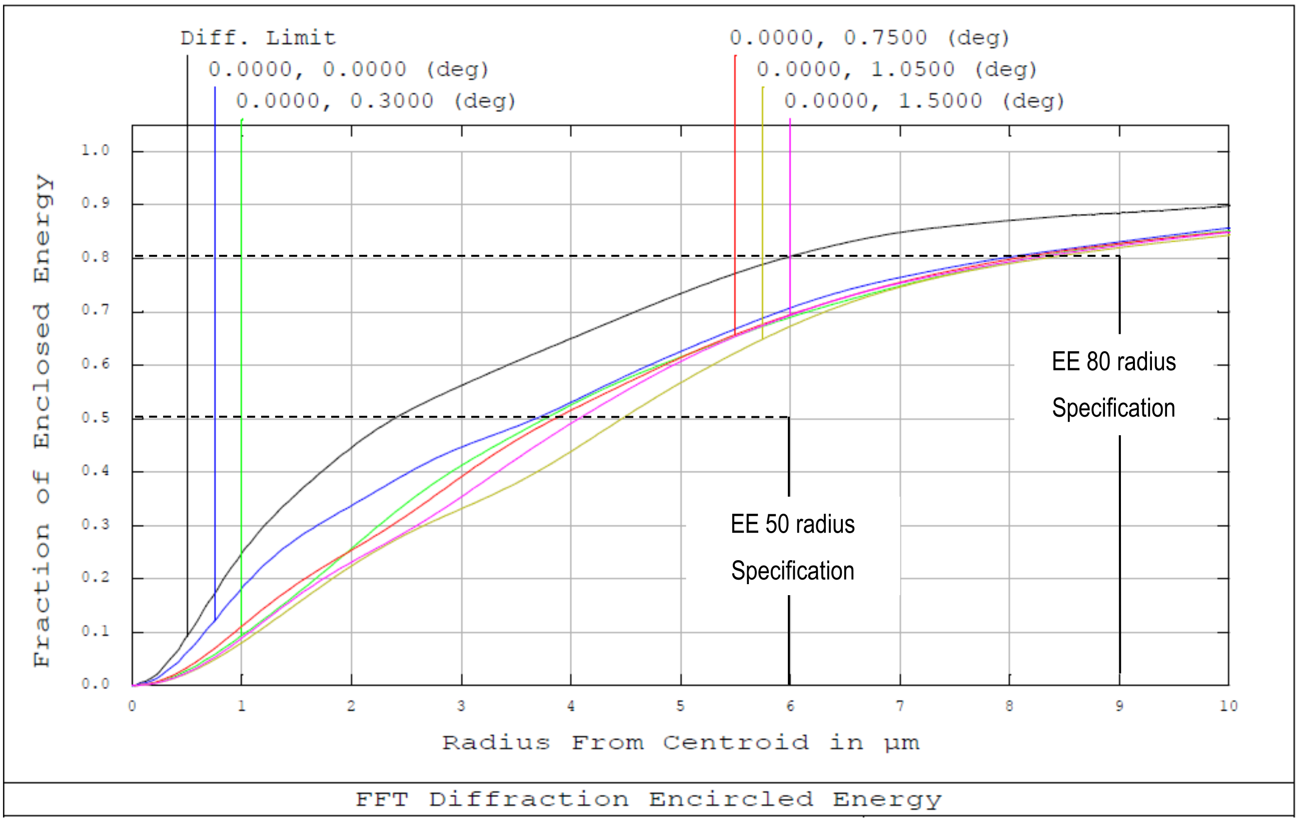


Figure 2. Polychromatic diffractive encircled energy

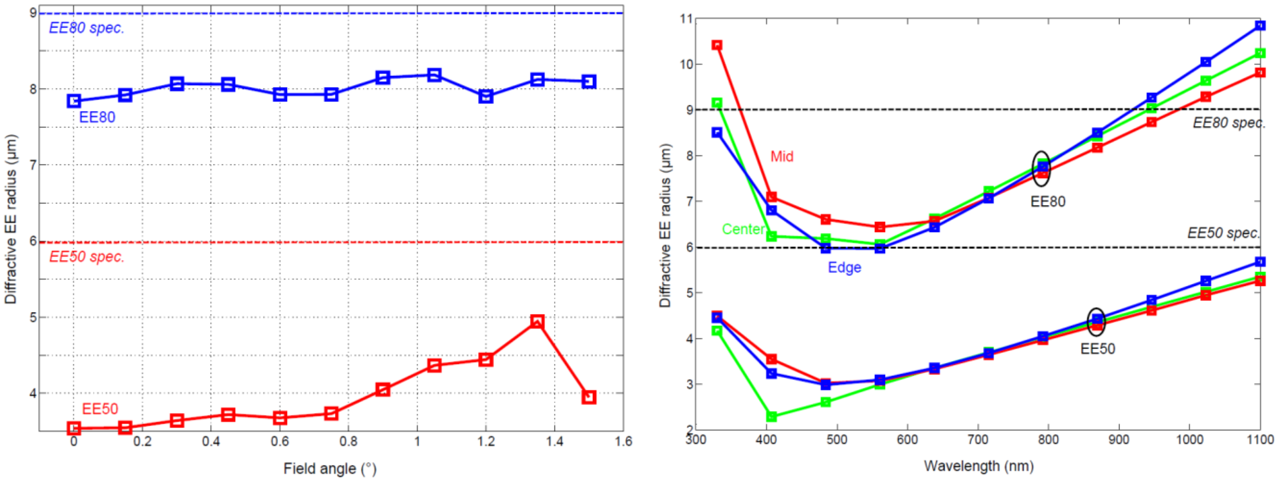


Figure 3. Diffractive EE50 and EE80 radius vs. the half field angle (right) and vs. the wavelength (left)

### 3.2 M1 Unit

The primary mirror is mounted on a passive support. It consists in a 36 points axial whiffle tree combined with 32 astatic lateral levers. The first and second stages of the whiffle tree are composed of bipods. The third stage is composed of tripods. The cell aims at maintaining the mirror image quality together with a very high stability regardless the operational conditions. AMOS has a proven experience in producing high performance 2 m class mirror with this kind of support. However, making a new support always requires a comprehensive analysis.

The FEM analysis of the mirror support provides the WFE performances for the nominal support under gravity, wind and thermal load. Then, the WFE sensitivity is evaluated for each contributor that produces parasitic forces and moments applied to the mirror. The tolerancing of the mechanical parts, the balancing accuracy of the whiffle tree and the adjustment accuracy of the astatic levers are derived from an error budget constructed on the basis of the sensitivity analysis. At the end, the consolidated error budget is not higher than 42 nm RMS WFE for the M1 unit including the mirror fabrication.

The primary mirror is manufactured at AMOS. After conventional polishing, the modern technique of computer controlled polishing is used for converging rapidly to the final shape. At the end of the manufacturing, the mirror is tested in its cell, on the axial support.

The M1 cell has been integrated at AMOS with a dummy mirror having representative mass characteristics and mechanical interfaces allowing a complete validation of the integration sequence. The performance of the support is insured by an accurate calibration of the astatic lateral levers and a proper balancing of each stage of the axial whiffle tree.

Figure 4. M1 mirror on polishing support (left) and M1 unit with dummy mirror before integration in telescope (right)

### 3.3 M2 Unit

Likewise M1, the secondary mirror is mounted on a passive support. It consists in a 18 points – 2 stages whiffle tree combined with a central membrane acting as the lateral support. The design elaborated by AMOS is compact and lightweight without impairing the performance of the support. The fact that the center of gravity of the M2 unit is remarkably close to the hexapod mounting interface contributes largely to the good performance of the hexapod implemented for the M2 active control.

Figure 5. M2 cell without mirror (left) and under test with dummy mirror (right)

The M2 unit has been mounted, adjusted and fully characterized before shipment to the M2 mirror manufacturer. The final acceptance of the mirror will be made inside the M2 cell.

The secondary mirror is fabricated by Brashear, USA. The fabrication process largely makes use of magnetorheological finishing (MRF) technology. The mirror test set-up consists of an off-axis Hindle test where the mirror is rotated around its axis to address 16 overlapped portions of the surface. The full phase map is reconstructed by stitching the 16 individual measurements. The consolidated error budget for the M2 unit is 40 nm RMS WFE including fabrication, supporting and thermal load.

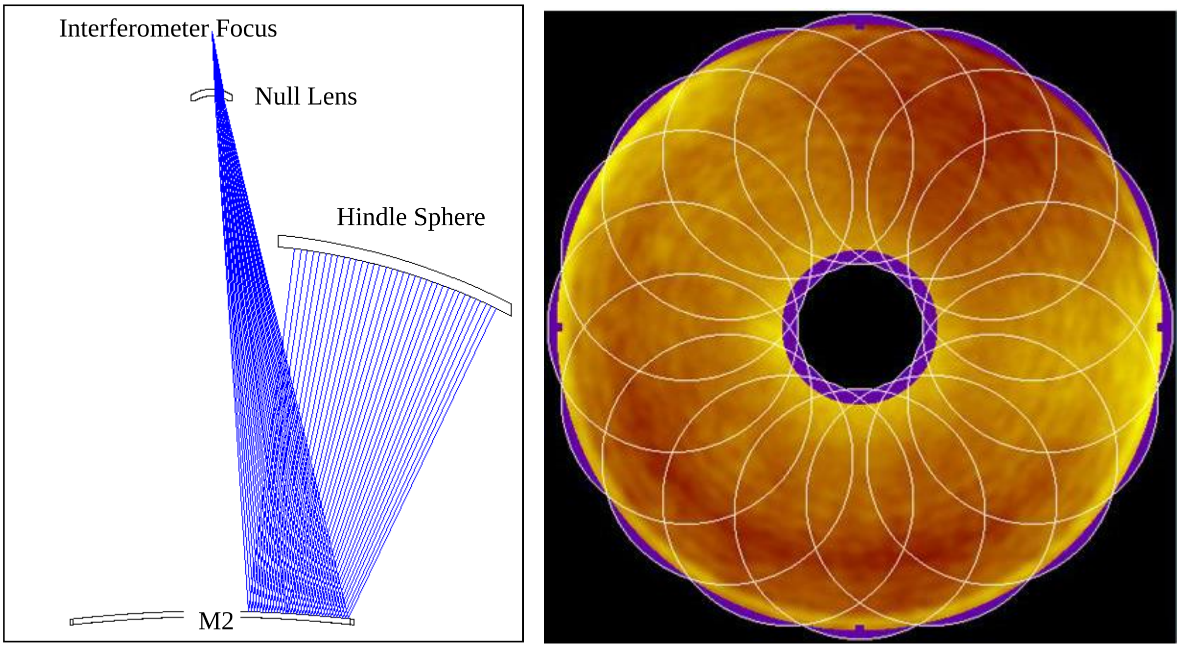


Figure 6. M2 mirror test set-up (left) and stiching scheme (right)

### 3.4 Field Corrector

The field corrector is the most challenging optical sub-system of the JST. It is composed of 3 lenses and a barrel for a total weight of 430 kg. Its contribution to the telescope image quality degradation is less than 90 nm RMS WFE in any operational conditions. The complete system is manufactured, assembled and tested by Tinsley, USA.

Although the optical design process aims at keeping the manufacturability of the lenses feasible, maintaining the best image quality in a large field of view leads to an exotic design: very short radius of curvature combined with high order aspheric prescription produce uncommon slope and change of slope along the radius of the lenses.

The complex shape of the lenses makes the system also more sensitive and requires very tight tolerances as well as very high stability over the lifetime. This sensitivity required to implement a thermally compensated support and almost gravity invariant. Lens L2 and L3 are tangentially supported in a stainless steel barrel. The lens L1 is supported by a passive hexapod made of Invar® rods. The hexapod also provide the adjustment capabilities necessary to position L1 with respect to the L2-L3 barrel.

The three lenses are produced independently of each other. The spherical surfaces are interferometrically tested while non-contact probing technology is used for testing the aspheric surface down to 40 nm RMS. The three lenses are mounted in the barrel and mechanically aligned by iterative CMM measurement. Then, the complete system is interferometrically tested in a null test where a collimated beam through the field corrector (double pass). Depending on the results of the test, the first surface of L1 can be reworked to correct low frequency defects. The high and medium frequency defects are characterized and controlled by the measurements of the individual lenses.

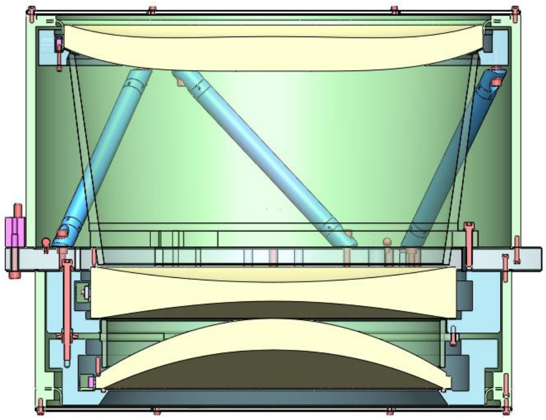

Figure 7. Field corrector optical opto-mechanical design (left) and non-contact probing (right)

### 3.5 Stray Light Mitigation

By nature, the short focal length and the wide FOV multiplies the possibility of having stray light reaching the focal plane. Baffles are foreseen to prevent rays from stars out of the FOV to reach the detector, while not inducing significant vignetting in the FOV. A stray light analysis performed in FRED optical software suggests a baffling set between M1 and M2 comprising 3 conical baffles so as to block all perturbing light resulting either from direct glimmer on the detector or unwanted reflection on M1 and M2. The FC is also baffled between L1 and L2 and between L2 and L3.

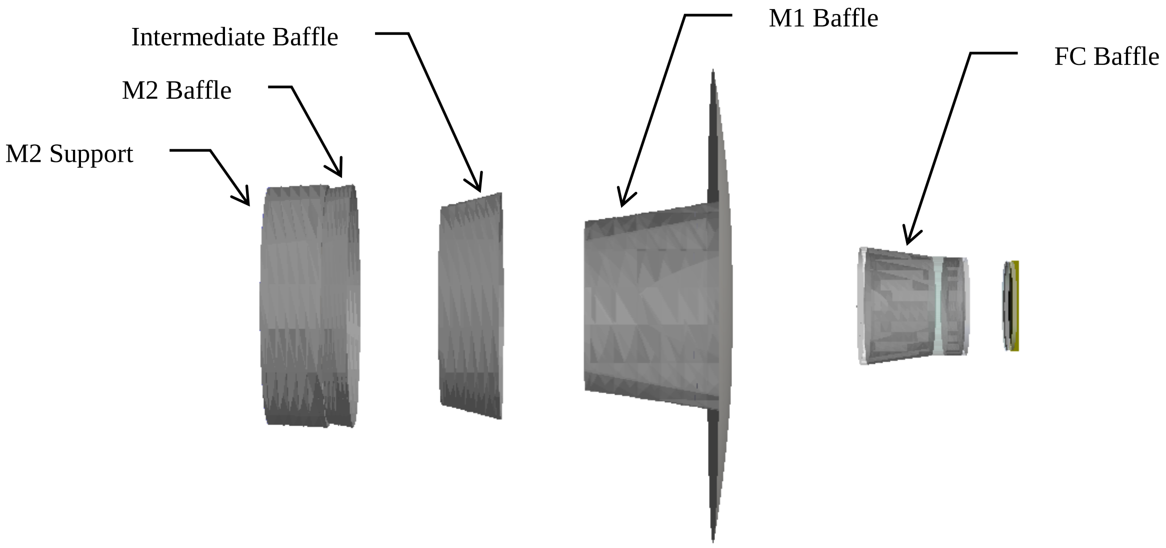


Figure 8. Baffling design

The mirror baffles are made of epoxy/carbon fiber composite material to provide the highest rigidity for a given geometry imposed by the optical design. The baffles are coated with a black paint that exhibits a very low reflectivity and a high surface roughness in order to spread the non-absorbed light in all the directions.

The implementation of grooves and vanes inside the baffles prevents specular reflection on the baffle surface to reach the detector. The decision of adding grooves is motivated by a quantitative analysis of the scattered light of the baffle surface and edges.

In addition to the stray light analysis, ghost images analysis has been conducted in order to validate the design regarding the impact of the ghost reflection compared to the sky background noise.

Far more than the reflectivity of the CCD ships, it was pointed out that the use of different dichroic filters produces pupil ghosts over a large portion of the detector regardless the optical configuration of the field corrector. This fact constrained the J-PAS to design advanced stacked filters and elaborate *ad hoc* observation strategies [2].

## 4. MOUNT DESIGN

The mount is also a key element for the performance of the telescope. By appropriate design, analysis and component selection, the JST mount offers the best static and dynamic performances. It guarantees the stability and surface quality of the optics. Its good dynamic behavior combined with a proper control system allows to attain utmost pointing and tracking performance.

The Alt-Azimuth mount is compact and structurally very stiff. The box frames structure exhibits natural frequencies not lower than 10 Hz. The Az bearing and the Alt bearing configurations largely contribute to these good performances. The first one is a three row roller bearing slewing ring. It connects the ground interface structure (GIS) to the fork. The second is composed of two pairs of preloaded high accuracy angular contact ball bearings that links the tube to the fork.

The main motors are rotary direct drives. Their intrinsic qualities contribute to the good performances of the system: no irregularities in the motion due to the gear geometrical imperfections, no backlash, no stick-slip effect at tracking speeds and no friction originating from the drive. They are coupled to multiple head high resolution encoders.

The weight of the complete telescope is approximately 45 tons. It is installed on a 10 m high concrete conical pier. The overall height from the pier is less than 7 m thanks to the short M1-M2 spacing.

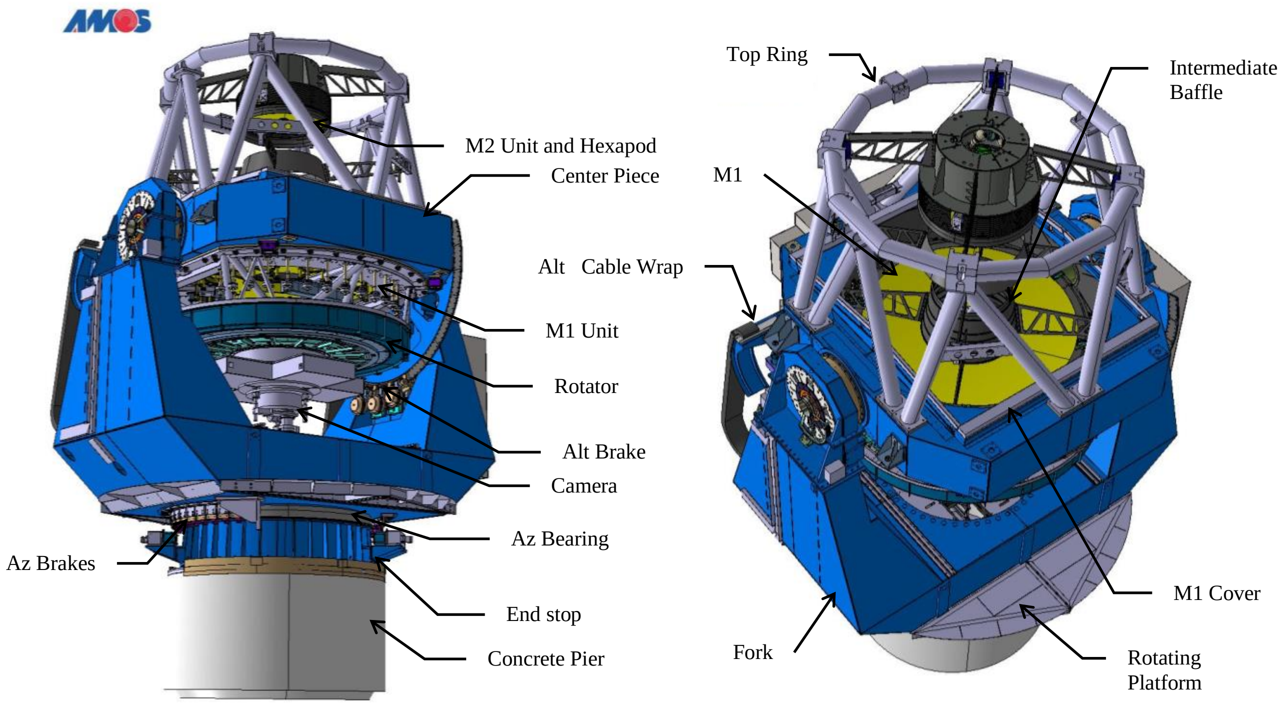


Figure 9. JST telescope – general views

The secondary mirror is mounted on a hexapod mechanism that provides the ability to periodically adapt the M2 position such that the image quality is always optimal in any operational condition. The M2 active system is designed to work in open loop as well as in closed loop as described in Section 5.3. The Hexapod delivered by Symétrie, France, has an accuracy better than 1 µm in focus over small travel ranges and a measured unidirectional resolution better than 0.1 µm.

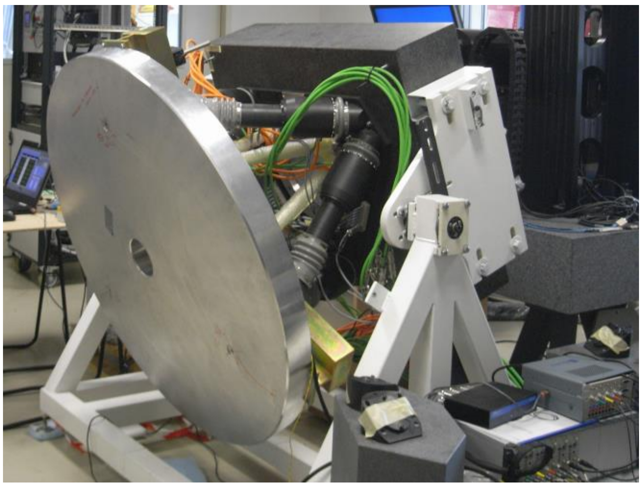

Figure 10. Hexapod under factory test with dummy M2

Figure 11. Instrument rotator - view from telescope side

The rotator is a masterpiece of the system in terms of complexity. It aims at supporting a 1.25 ton camera while compensating for the field rotation. It includes two symmetrical cable wraps to bring power, cooling, etc. to the instrument. The large size of the focal plane requires unusual tracking accuracies. It was therefore necessary to implement an axis configuration similar to that of the Az axis: a direct drive motor inside a three-rows roller bearing slewing ring. The field corrector is installed inside the rotator and is connected to its fixed part while the camera is directly connected to the slewing ring bottom face.

The tracking performances and the bandwidth of the main axes are evaluated by means of a SIMULINK® model. The model includes the U-MAC controller, the motors, the encoders and a state-space MIMO model of the axis. The latter is constructed from identified transfer functions and the friction model that converts the velocity of the motors into a counter-reaction torque applied to the structure.

The image motion resulting from the mirrors displacements and the axis angular position are evaluated as a function of i.) the unitary motor torque and ii.) the normalized wind pressure field applied to the telescope structure. The FEM transfer functions are then analytically identified and incorporated to the model.

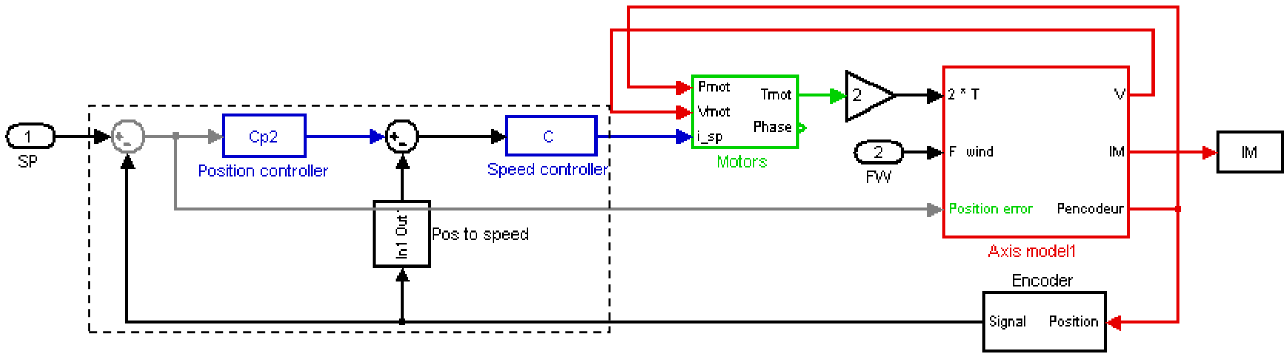


Figure 12. Altitude axis dynamic model

## 5. CONTROL SYSTEM

### 5.1 Telescope Control System

The control system architecture is largely inspired from one adopted for all the latest telescopes build by AMOS.

As presented in Figure 13, the tasks of the telescope control system are handled by two major systems: one Linux PC and an industrial programmable logic controller (PLC).

The Linux PC is dedicated to the astrometric calculations, the graphical user interface (local and remote), the auto guiding, the M2 active control and the control of the time related axes (azimuth, altitude and rotator). The TCS PC feeds the Delta-Tau UMAC controller with axes position in an absolute time frame generated by the embedded GPS card. The Linux-based TCS application is developed under NI-LabVIEW.

The communication between TCS and the other entities uses an ASCII protocol through a socket server. Hence, all the TCS functionalities can be implemented in a third party application and the telescope can be operated through an additional layer or GUI. The engineering mode of the TCS can be run in the local GUI exclusively while the operational mode can be run on a remote computer.

The PLC handles all the tasks related to the control of the safety devices, the auxiliary axes as the M1 cover, the thermal control, etc. It also manages the communication with the observatory infrastructure, the air conditioning and the dome control system. A PROFIBUS® is deployed for the communication between the PLC and external entities.

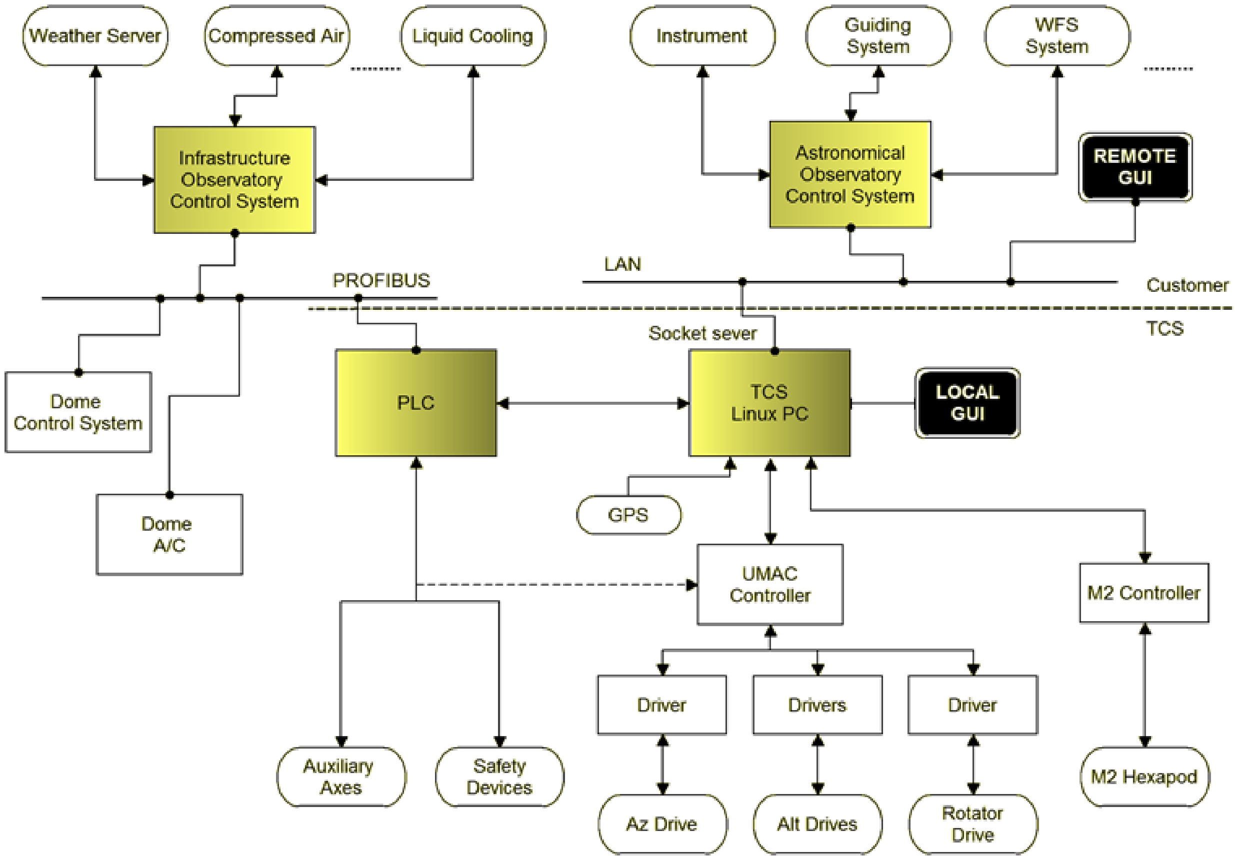


Figure 13. Telescope control system architecture

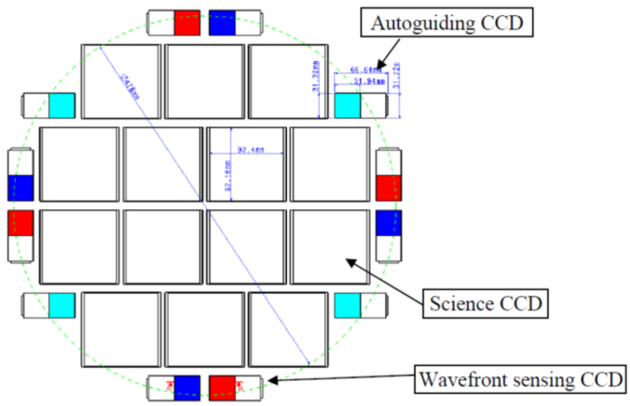


Figure 14. Camera focal plane configuration

Both the tracking performances and the image quality are preserved by implementing active closed loops. For the two of them, additional sensors are built-in the camera and provide feedback to the telescope control system. They are positioned at the edge of the field of view without encroachment of the sciences CCD area.

As explained here after, four CCD provide simultaneously four guiding stars feedback to the TCS. In the same way, four pairs of CCD allow to calculate the image quality at four locations of the FOV and provide four sets of Zernike coefficients to the TCS.

### 5.2 Guiding System

Developing an auto guiding control loop for a wide field telescope is not as straightforward as for a conventional telescope. At first, the science CCD configuration in the camera allows only to pick-off external portions of the field of view despite the tracking performances are usually evaluated on the optical axis. Secondly, the differential atmospheric refraction between two stars distant of 1.5 deg becomes significant at elevation lower than 45 deg. Finally the wavelength difference between the science CCD and the guiding CCD's must be taken into account. It is therefore necessary to develop an adequate strategy to deal with these constraints.

Four auto-guiding auxiliary CCD's installed in the focal plane provide centroid position of guide starts continuously to the TCS when the closed loop mode is activated.

In order to minimize the tracking error across the FOV, four virtual telescopes are implemented in the TCS. Starting from the Ra-Dec coordinates derived from the measured (X,Y) initial position of a guide star in the FOV and the central wavelength of the guiding CCD, the virtual telescope computes the successive expected guide star positions and compare them with the following measured positions provided by the guiding CCD. If four guide star positions are available, a solid body linear fit can be applied to the set of measured and expected positions. The results of this fit provides the estimation of the (X,Y) shift of the center of the FOV and a rotation angle corresponding to the instrument rotator correction. The process is working similarly with three or two guide stars. If the data of only one guide star are usable, no rotation can be corrected.

### 5.3 M2 active control

Maintaining the image quality in any operational condition requires compensating the relative movement of the optics by an adjustment of the M2 mirror position thanks to the hexapod mechanism. In open loop operation, the focus, tip-tilt and decenter position of the M2 are given as a function of the elevation angle and the temperature:

$$A + B.\ cos(alt) + C.\ sin(alt) + D.\ (T\text{-}T_0) + uoffset$$

While tracking, the TCS continuously computes the M2 correction and apply it when the corresponding image quality degradation is higher than a predefined threshold.

Above the open loop correction, a closed loop mode is using wavefront sensor feedback to update the M2 position. In order to provide continuous truthful feedback without perturbation of the observation, it was proposed to implement four curvature wavefront sensors inside the focal plane. Each sensor is composed of two CCD's located 1 mm above and below the science CCD plane and provide respectively intra-focal and extra-focal images of two neighboring stars.

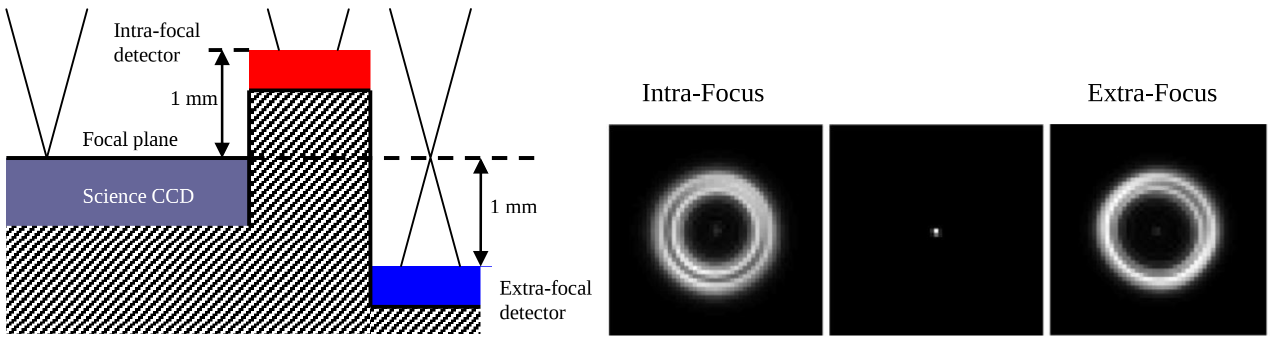


Figure 15. Curvature wavefront sensor configuration and corresponding star images scaled to the CCD pixel size (9 µm)

From the acquisition of the out-of-focus images, the curvature sensing system must reconstruct the wavefront at the exit pupil of the telescope, and particularly characterize its Zernike polynomial decomposition, so as to enable the correction of the aberrations by appropriate hexapod motions. When using such corrections with an hexapod, only the low-order aberrations may be suppressed independently, these are the focus (Zernike coefficient Z4), astigmatism (Z5 and Z6) and coma (Z7 and Z8). That represents 5 aberrations to correct from the 5 degrees of freedom of the hexapod. In addition to this correction, focus measurements at the edge of the FOV provide additional information regarding the global tilt of the focal plane.

Four curvature wavefront sensors are built-in the camera and provides four sets of Zernike coefficient that are passed to the TCS. Since the image quality is not homogeneous across the FOV and depends on the frequency range, one cannot simply try to optimize the image quality across the field of view on the basis of one single measurement. An ideal initial state of Zernike decomposition at the edge of the FOV will be determined for each science CCD's - filter combination. The optimum correction that recovers almost the initial state can be achieved only by using the four sets of Zernike data.

## 6. ASSEMBLY, INTEGRATION AND TEST

The verification of performances and functionalities follows a strict plan. The main components such as the optics, the hexapod, the TCS, etc. are tested at supplier factory according to a test procedure approved by AMOS. In the meantime, the telescope is assembled and the sub-systems are integrated. Intermediate tests and alignment are achieved to guarantee that the telescope is in perfect operational condition before proceeding to the test. The functionalities and the interfaces are tested before proceeding to the performance tests or factory acceptance tests (FAT).

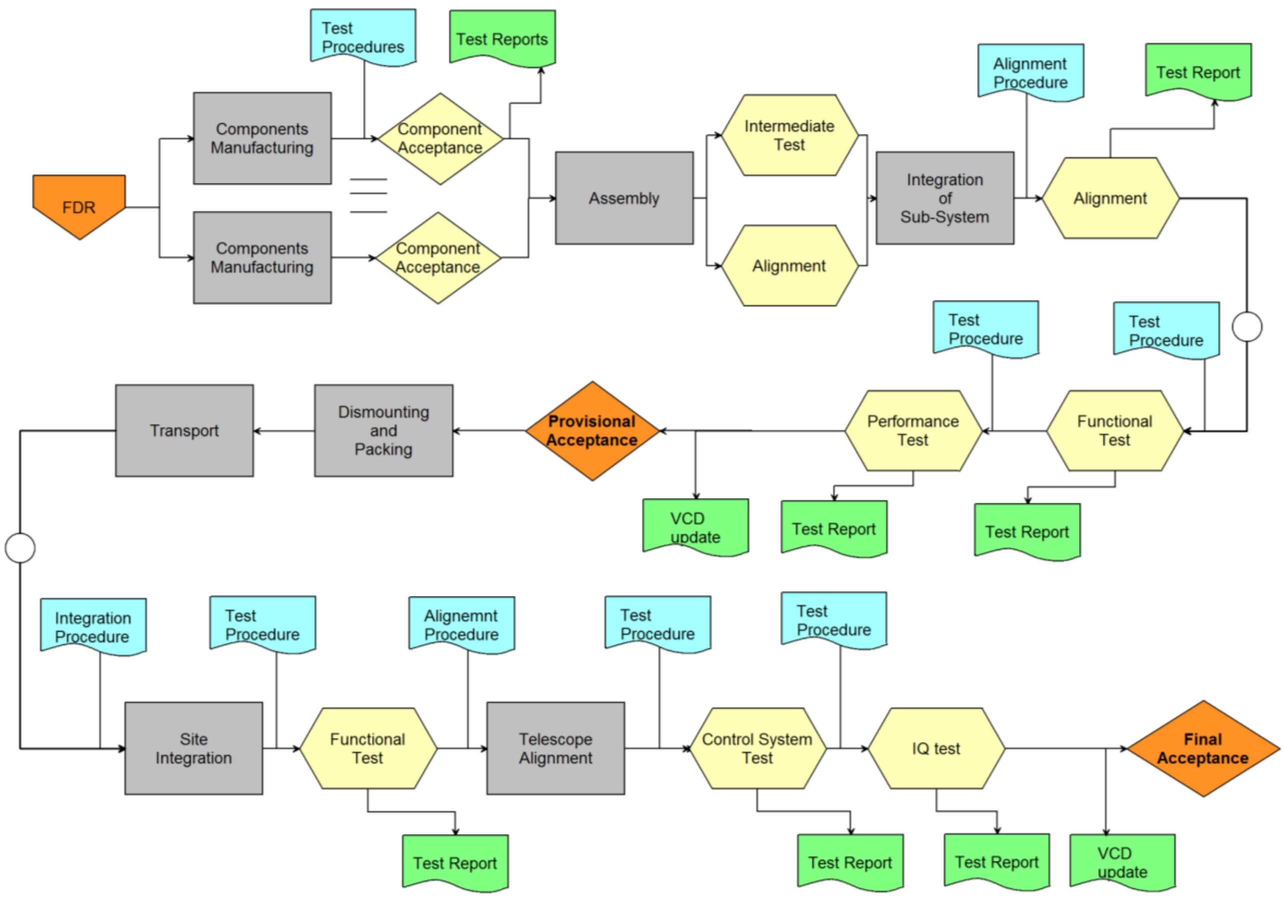


Figure 16. JST test plan

After the FAT, the telescope is dismounted and transported to the site. The on-site integration is followed by functional tests and optics pre-alignment leading to the first light. A verification camera equipped with two CCD is provided for that purpose, as well as for achieving the final acceptance tests. The pointing and tracking performances are tested in the first phase of the site acceptance. A good pointing model is built for that occasion. The image quality is tested in the second phase after the validation and possible enhancements of the M2 active control open loop model.

Figure 17. JST integration at AMOS

## 7. CONCLUSION

Astronomical survey programs bring the time as the ultimate constraint for the design of telescopes and instruments. The throughput is quantified in term of time to complete the in-depth survey of the accessible portion of the sky for a given wavelength range. All the specifications of the telescope result from this goal and lead to increase the field of view without impairing any performance of the system.

AMOS has acquired a valuable experience in making telescope since 30 years and largely uses it in the frame of the Javalambre Survey Telescope Project. A highly qualified multidisciplinary team was set to conduct the project to the success. AMOS makes use of the most advanced analysis techniques, machinery and instrumentation in all areas of work to produce a state of the art telescope that fully fulfills the expectations of the end-user.

## REFERENCES


[1] Cenarro, A. J., et al., "The Observatorio Astrofísico de Javalambre: Goals and Current Status," Proc. SPIE 8448 (2012).

[2] Marín-Franch, A., et al., "Design of the J-PAS and J-PLUS filter systems," Proc. SPIE 8450 (2012).

[3] Yanes-Días, A., et al., "Goals and strategies in global control design of the OAJ robotic observatory," Proc. SPIE 8451 (2012).